Micelles of Polysoaps: The Role of Bridging Interactions

O. V. Borisov

Institute of Physics, Johannes Gutenburg University, 55099 Mainz, Germany

A. Halperin*

CRPCSS, 24 av du President Kennedy, 68200 Mulhouse, France

Received October 23, 1995[⊗]

ABSTRACT: Polysoaps, hydrophilic polymers incorporating amphiphilic monomers, form intrachain micelles in aqueous media. The micelles are similar to those formed by monomeric amphiphiles but are also endowed with a swollen, starlike corona formed by the spacer chains joining the amphiphiles. Long polysoaps form strings comprising many intrachain micelles. Exchange of amphiphiles between such micelles may give rise to bridging attraction, resulting in the adoption of a collapsed configuration in which the swollen micelles are close packed into a spherical globule. Upon addition of free amphiphiles, this structure unravels in a highly nonlinear fashion. Titration by surfactants, and the resulting swelling, provide information about the configurations of the dilute polysoaps.

I. Introduction

Hydrophilic polymers incorporating, at intervals, amphiphilic monomers form intrachain micelles in aqueous media.[1,2] The interior of such micelles is similar to that of micelles formed by short-chain amphiphiles. They comprise hydrophobic cores of hydrocarbon tails with polar or ionic head groups straddling the interfaces. However, the exterior of the intrachain micelles exhibits a new feature: a swollen corona of loops formed by the spacer chains (Figure 1) joining the aggregated amphiphiles.[3] In turn, the corona modifies the equilibrium structure of the micelle, their interactions, and their kinetics of equilibration. The configurations of such polymers, "polysoaps", are strongly affected by the intramolecular aggregation. Also affected is the interaction between the polysoaps and monomeric, free surfactants. The configurations of the polysoaps are determined by the overall polymerization degree of the chain, N, the number of amphiphilic monomers incorporated into the chain, m, and the characteristics of the amphiphilic monomers. When N and m are large enough, each polysoap chain can form many intrachain micelles. Little is known of the overall configurations of such strings of micelles. When the intrachain micelles are spherical, it is possible to envision three extreme scenarios (Figure 2): (i) a linear string of micelles,[3] (ii) a branched string of micelles,[3] (iii) and a *collapsed* globule of micelles (*i.e.*, close-packed, spherical globule of swollen micelles). This last case is expected when the micelle−micelle interactions are *attractive*. The second case corresponds to the equilibrium configuration when the micelles repel each other. The first case may be favored by the kinetics of aggregation when the micellar interactions are repulsive. At present, there is no clear evidence favoring one scenario over the others. Experimental studies[4] do however suggest that polysoaps may undergo configurational changes over very long periods of time. As we shall argue, kinetics are indeed expected to play a crucial role in the selection of the realized configurations. In view of this, it is of interest to explore the different scenarios and their experimental signatures. Clearly, the three scenarios result in different chain dimensions. They also give rise to a different dependence of the equilibrium chain dimensions, R_{eq}, on the concentration of free amphiphiles, X. This dependence is due to the incorporation of free amphiphiles into the intrachain micelles (Figure 1). In turn, this leads, eventually, to complete unfolding of the chain with corresponding increase in its dimensions. As we shall argue, the R_{eq} *vs* X curves should provide useful evidence on the configurations adopted by the dilute polysoaps. In the following, we focus on the third scenario and its signatures. Within this scenario, the micelles attract each other because of *bridging* resulting from the *exchange of amphiphiles* between them (Figure 3). Our discussion is confined to dilute solutions of noninteracting polysoaps forming spherical intrachain micelles. The hydrophilic spacer chains considered are neutral, flexible, and of low

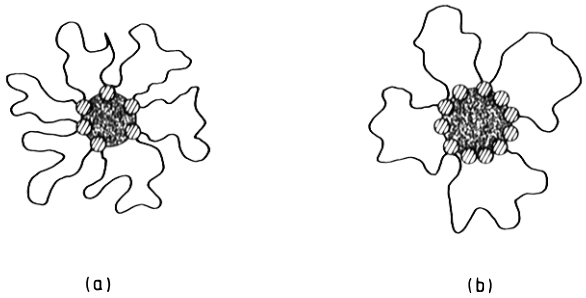

Figure 1. Schematic cross section of pure (a) and mixed (b) intrachain micelles. The formation of mixed micelles lowers the numbers of loops per micelle and thus the associated free energy penalty.

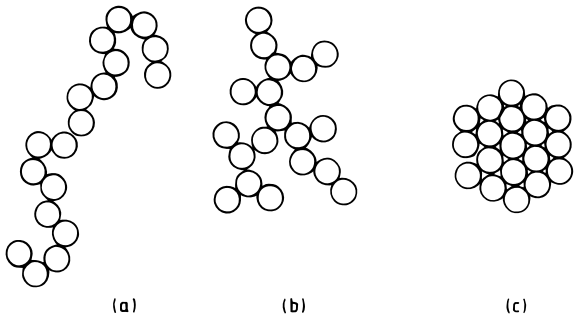

Figure 2. Three extreme configurational scenarios considered for polysoaps: (a) linear chain of micelles: (b) a branched chain; (c) a collapsed globule of close-packed swollen intrachain micelles. Intermediate scenarios are also possible.

[⊗] Abstract published in *Advance ACS Abstracts,* February 15, 1996.

0024-9297/96/2229-2612$12.00/0

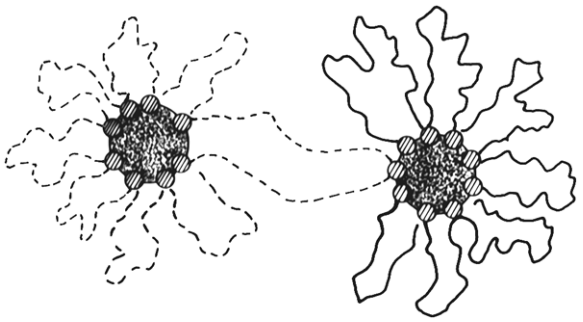

Figure 3. Bridging attraction between two intrachain micelles due to exchange of amphiphiles between them.

polydispersity. Furthermore, water is assumed to be a good solvent for the hydrophilic chains. The discussion is further limited to solutions of high ionic strength when long-range electrostatic interactions are screened. For simplicity, the free surfactants are chosen to be identical to the amphiphilic monomers incorporated into the chain. The discussion is limited to systems in which the free amphiphiles do not adsorb on the spacer chains. Finally, we focus on the case of long spacer chains *i.e.*, $1 \ll m \ll N$. The following questions are addressed: (i) What is the dependence of the polysoap equilibrium size, R_{eq}, on N and m? (ii) How does R_{eq} vary with the concentration of free surfactants, X?

The theory of bridging interactions[5−12] has been studied extensively in the past. The work dealt primarily with the formation of physical mesogels and with the interactions between flat surfaces. In the following, we focus on the effect of bridging interactions on the *configurations* of isolated polysoaps. The bridging attraction gives rise to a *negative* second virial coefficient, $B < 0$. This suggests that the isolated polysoaps adopt the configuration of a collapsed globule and that phase separation between a dilute solution and a denser physical gel takes place. However, as we shall argue, it is necessary to allow for the dynamics of bridging. As opposed to monomer−monomer attraction in poor solvents, bridging interactions are not instantaneous. Since the bridging is an *activation process*, long-lived, metastable configurations which are free of bridging are possible. This last point is of fundamental interest since it suggests that the free energy surface characterizing the configurations of polysoaps exhibits *multiple minima*. Another novel feature concerns the formation of mixed micelles incorporating both free and polymerized amphiphiles. In this system, a novel driving force, the *decrease* in the *coronal penalty*, comes into play.

These issues are of interest from two perspectives. First, polysoaps and the related hydrophobically modified water-soluble polymers are of practical importance as viscosity modifiers.[1,2] These associating polymers are used in the cosmetics, paints, and paper industries in order to adjust the flow properties of fine solid dispersions. Their utility is due to their shear thinning behavior, which is attributed to the formation of weak physical gels. The understanding of the viscoelasticity of such gels is only possible once the configurational and elastic properties of the polymers are clarified. The second, more fundamental, perspective concerns the "secondary structure" of polysoaps and its effect on their configurations, elasticity, *etc.* The monomer sequence of the polysoaps, their "primary structure", gives rise to secondary/tertiary structure due to their internal micellization. This in turn modifies their behavior. These modifications have no counterparts among simple homopolymers and even among simple associating polymers such as telechelic chains. On the other hand, these features are reminiscent of biopolymers and, in particular, proteins. These qualitatively novel effects are thus of inherent interest within the framework of both polymer science and the biophysics of biopolymers.

The article is organized as follows. A model of the intrachain micelles is briefly summarized in section II. The bridging interactions are discussed in section III. The discussion focuses on the thermodynamic aspects of bridging but also touches on kinetic aspects. Finally, the effect of bridging on the equilibrium configurations of polysoaps is considered in section IV. The interactions between free surfactants and isolated polysoaps are also considered in this section.

II. A Model of Intrachain Micelles

Since polysoaps incorporate amphiphilic monomers, it is natural to use micelles formed by the free, unpolymerized surfactants as a reference system. Furthermore, it is legitimate to ignore long-range electrostatic interactions between the micelles because we focus on solutions of high ionic strength. With these observations in mind, we base the discussion of the intrachain micelles on a simple phenomenological model for free micelles.[13] Within this model, the free energy per amphiphile, in a micelle with an aggregation number q, $kT\epsilon_q$, consists of two terms. The first is due to the interfacial free energy of the core−solvent boundary. This term favors aggregation so as to minimize the interfacial free energy per amphiphile γkTa. Here γa is a dimensionless surface tension and a is the surface area per head group. The number of binary contacts between one head group and its neighbors is proportional to the surface density of the head groups, $1/a$. The associated term is thus kTK/a, where K is a constant to be determined. Altogether $\epsilon q \approx \gamma a + K/a$ and minimization with respect to a yields $\epsilon_q(\min) \approx 2\gamma a_0$, where $a_0 \approx (K/\gamma)^{1/2}$ is the optimal area per head group. It is thus possible to rewrite ϵ_q as $\epsilon_q \approx \gamma a_0(a/a_0 + a_0/a)$. This expression does not allow for the transfer free energy of the hydrocarbon tail from the aqueous environment into the core, $-\delta kT$. Strictly speaking, $\epsilon_q(\min) \approx 2\gamma a_0 - \delta$. We mostly ignore this constant term since it does not affect the equilibrium condition. It may however play a role in the interactions between free amphiphiles and the polysoaps. It is possible to incorporate this contribution into the expression for ϵ_q by rewriting it as

$$\epsilon_q \approx \ln X_c + \gamma a_0(a/a_0 + a_0/a - 2) \qquad (1)$$

where $X_c \approx \exp[\epsilon_q(\min)]$ is the critical micellar concentration of the free amphiphiles. X_c is then taken as an experimentally observable value which thus reflects the contribution of δ.

When micelles of free surfactants are considered, it is crucial to allow also for the loss of translational entropy upon aggregation. This contribution is clearly absent in the case of intramolecular aggregation. Instead it is necessary to supplement the free energy per surfactant by a third term[3] allowing for the coronal free energy penalty, F_{corona}. The aggregation forces the spacer chains to fold back and form loops. Since the area per head group is rather small, the loops crowd each other, giving rise to F_{corona}. F_{corona} supplements the head group repulsion in opposing micellar growth. An

intrachain micelle comprising of p polymerized surfactants is surrounded by p loops consisting each of $n \approx N/m$ monomers. In the following, we mostly focus on the starlike limit when the coronal dimensions, H, are large in comparison to the radius of the core, R_{core}. As a result, the overall micelle size is $r_{micelle} \approx H$. The structure of the corona is then similar to a star polymer with $2p$ arms each consisting of $n/2$ monomers; *i.e.*, the corresponding star is obtained by cutting each loop in half. The characteristics of the starlike corona, dimensions, concentration profile, and free energy per arm are well described by the Daoud−Cotton model.[14−17] Within this model, the corona is envisioned as a concentric array of shells of close-packed screening blobs. Each arm contributes a single blob to each shell. Thus, a shell of radius r and area r^2 consists of $2p$ blobs of cross section ξ^2, thus leading to $\xi \approx r/p^{1/2}$. Since $\xi \sim \phi^{3/4}$, the concentration profile is $\phi \sim r^{-4/3}$. H is determined by the requirement of monomer conservation $n \approx \int_{R_{core}}^{R_{core}+H} (\xi/b)^{5/3}\xi^{-1}\,dr$, where $(\xi/b)^{5/3} \approx g$ is the number of monomers in a blob of size ξ and b is a typical monomer size. The free energy per arm, as given by the kT per blob ansatz, is $F_{corona}/kT \approx \int_{R_{core}}^{R_{core}+H} \xi^{-1}\,dr$.

F_{corona} and H are thus

$$H/b \approx p^{1/5}n^{3/5}$$

$$F_{corona}/kT \approx p^{1/2}\ln(R_{core}+H)/R_{core} \approx p^{1/2}\ln n \quad (2)$$

The equilibrium structure of an intrachain micelle corresponds to a minimum of the free energy per polymerized surfactant[3]

$$\epsilon_p \approx \gamma a_0\left(\frac{a}{a_0}+\frac{a_0}{a}\right) + F_{corona}/kT \quad (3)$$

To proceed further, it is helpful to express F_{corona} in terms of the area per head group, a, and the volume of the hydrocarbon tail, v. For a spherical micelle comprising p amphiphiles $R_{core}^3 \approx pv$ and $R_{core}^2 \approx pa$, thus leading to $p \approx v^2/a^3$. Upon defining $p_0 \approx v^2/a_0^3$, we may rewrite F_{corona} as $F_{corona}/kT \approx p_0^{1/2}(a_0/a)^{3/2}\ln n$. Introduction of the dimensionless variable $u = (a_0/a)^3 = p/p_0$ allows us to express ϵ_p as

$$\epsilon_p/\gamma a_0 \approx u^{-1/3} + u^{1/3} + \kappa u^{1/2} \quad (4)$$

Here $\kappa \approx p_0^{1/2}\ln n/\gamma a_0 > 0$ is a dimensionless parameter measuring the relative importance of F_{corona} and the head group repulsion for $a = a_0$. When $\kappa \ll 1$, the coronal contribution is negligible and the micelles retain the characteristics, a_0 and p_0, of micelles formed by free surfactants. In the opposite limit, $\kappa \gg 1$, the coronal penalty is dominant and the intrachain micelles at equilibrium are smaller; *i.e.*, $a_{eq} > a_0$ and $p_{eq} < p_0$. The equilibrium micellar structure is determined by $\partial\epsilon_p/\partial u = 0$ or

$$u_{eq}^{2/3} + \kappa u_{eq}^{5/6} \approx 1 \quad (5)$$

When $\kappa \ll 1$, the coronal contribution is negligible and the second term may be ignored, thus leading to $u_{eq} \approx 1$ or $a_{eq} \approx a_0$ and to $p \approx p_0$. Accordingly, the micellar size, $r_{micelle}/b \approx p_{eq}^{1/5}n^{3/5}$, is

$$r_{micelle}/b \approx p_0^{1/5}n^{3/5} \quad (6)$$

On the other hand, when $\kappa \gg 1$, the first term is negligible and thus $\kappa u_{eq}^{5/6} \approx 1$, leading to $u_{eq} \approx \kappa^{-6/5}$ or

$$p_{eq} \approx p_0\kappa^{-6/5} \approx p_0^{2/5}(\gamma a_0/\ln n)^{6/5} \quad (7)$$

The micellar size in this limit is

$$r_{micelle}/b \approx p_0^{2/25}n^{6/25}(\gamma a_0/\ln n)^{6/25} \quad (8)$$

III. On Bridging Interactions

It is possible to estimate the strength of the equilibrium bridging attraction between micelles within the framework of the Daoud−Cotton[14] model. The argument proceeds as follows. First, the coronas of two micelles can interpenetrate up to a depth comparable to the outermost blob, $\xi_0 = \xi(H) \approx H/p^{1/2} \approx n^{3/5}p^{-3/10}b$. The free energy penalty associated with such overlap is comparable to kT. The corresponding contact area is $A \approx H\xi_0$. Stronger interpenetration is unlikely because the resulting free energy price is much higher, $F/kT \approx p^{3/2}\ln H/D$, where D is the distance between the two micellar centers.[18] Second, one may argue that the density of bridges is proportional to the density of loop midpoints in the overlap region.[12] Within the Daoud−Cotton model, the midpoints are all localized in the coronal periphery. Each ξ_0 blob contains one end, and the surface density of the ends at the overlap region is thus ξ_0^{-2}. Finally, we assign each bridge an attractive free energy of kT. The total bridging free energy between two micelles, ΔF_b, is thus

$$\Delta F_b/kT \approx -A/\xi_0^2 \approx -H/\xi_0 \approx -p^{1/2} \quad (9)$$

The intermicellar potential, U, reflects the combination of the bridging attraction and the osmotic repulsion discussed above. To obtain the corresponding second virial coefficient, B, we approximate U as a square well of width ξ_0 and depth $|\Delta F_b|$ having an infinite wall at $H - \xi_0$. Upon substitution in $B = \int_0^\infty [1 - \exp(-U/kT)]r^2\,dr$, this leads to

$$B \approx H^3 - H^2\xi_0\exp(|\Delta F_b|/kT) \quad (10)$$

The first term reflects the excluded volume interactions between the "hard repulsive walls" representing the osmotic repulsion. The second, negative, term accounts for the bridging attraction. The second term is dominant whenever $|\Delta F_b|/kT > \ln(H/\xi_0)$ or $p^{0.5} > \ln p^{0.5}$ as is the case when $p > 1$. As a result, B is negative in this regime.

The argument presented above relies on the Daoud−Cotton model—in particular, on two ingredients: the predicted concentration profile and the assumed localization of the ends at the coronal periphery. Both are confirmed by computer simulations[19] as well as by numerical SCF calculations.[20,21] The two methods reveal an extended inner region exhibiting $\phi \sim r^{-4/3}$. Furthermore, the ends are excluded from an interior "dead zone" of width comparable to H. The ends exhibit a Gaussian distribution consistent with the fluctuations of the end-to-end vector of a chain confined to a conical capillary. A purely analytical SCF theory of stars is yet to be developed. An approximate SCF description based on the results quoted above was recently proposed.[21] Within this description the corona is assumed to consist of two concentric regions: an inner "dead zone" containing no ends, and an exterior, thin region which is similar to a flat brush *i.e.*, is characterized by a parabolic profile.

One should note however that for extended coronas the concentration profile and the end distribution obtained by this approach do not agree well with the results obtained by simulations and numerical methods. Yet, this approach allows for more rigorous analysis of the bridging attraction.[12] The main results obtained by this method are recovered by the simple argument presented earlier. The main difference is that $\Delta F_b/kT \sim p^{3/10}$ rather than $\Delta F_b/kT \sim p^{1/2}$ and, consequently, $B < 0$ whenever $p^{0.3} > \ln p^{0.3}$.

The preceding discussion focused on the thermodynamics of the bridging attraction. However, bridging, as opposed to monomer−monomer interactions, is not instantaneous. The exchange of amphiphiles between the micelles is an activation process that may be slow in comparison with the residence time of the micelles within the interpenetration distance $2(H - \xi_0)$. Two activation energies come into play during the exchange process. One is δkT, the transfer free energy of the hydrophobic tail from the core into the aqueous environment. The second is the insertion free energy of the spacer chain into the second corona. An upper bound for the insertion activation free energy is simply $kTp^{1/2} \ln n$, the excess free energy of an arm in the corona as compared to a free chain. This estimate is based on the assumption that the expulsion of the amphiphile takes place before the micelles come into contact. The height of this barrier is reduced when the expulsion occurs while the micelles are in contact. In such a case, the spacer chain is expelled into a semidilute solution with $\xi \approx \xi_0$. The reduced activation free energy is then $kT(p^{1/2} \ln n - n/g_0) \approx kTp^{1/2}(\ln n - 1)$, where g_0 is the number of monomers in a ξ_0 blob. A more rigorous analysis of the expulsion and the insertion processes is possible within the framework of a Kramers type rate theory.[22] However, for our purposes it is sufficient to consider the dominant contribution, due to the exponential effect of the activation barriers. This suggests that the characteristic time for bridging, τ_b, may scale as the longest of the following: $\exp(\delta)$, $n^{p^{1/2}}$, and $(n/e)^{p^{1/2}}$. These characteristic times should be compared to the residence time, τ_r, of the two micelles within the interaction distance, $2(H - \xi_0)$. τ_r may be identified as the time required by a micelle in order to diffuse a distance of ξ_0. Since the micellar diffusion coefficient scales as $D \sim 1/r_{micelle} \approx 1/H$, we obtain $\tau_r \approx D^{-1}\xi_0^2 \sim H\xi_0^2$ or $\tau_r \sim n^{9/5}p^{-2/5}$. While these estimates are very rough, they do suggest that $\tau_b \gg \tau_r$ is possible if not likely. In such cases the development of bridging between interchain micelles in a dilute solution may be very slow. This allows for long-lived configurations in which the micellar interactions are repulsive because of osmotic repulsion between the coronas. One should note that this is only the case while the micellar concentration is below the overlap threshold. Above this concentration the micelles are closely packed, τ_r is much longer, and bridging is thus much more likely.

On a more fundamental level, the activation processes described above are expected to play a role in any configurational rearrangement of the polysoaps. This, in turn, suggests that the free energy surface corresponding to the polysoap chain exhibits multiple minima.

IV. Configurations and Interactions with Free Surfactants

The negative equilibrium B suggests that the string of micelles adopts a globally collapsed configuration. The chain assembles into a spherical globule of close-packed, swollen micelles. The radius of the globule in $R_{eq} \approx (m/p_{eq})^{1/3} r_{micelle}$. Thus, for the $\kappa \ll 1$ limit, when $p_{eq} \approx p_0$ and the micellar radius is $r_{micelle}/b \approx p_0^{1/5} n^{3/5}$

$$R_{eq}/b \approx N^{1/3} n^{4/15} p_0^{-2/15} \tag{11}$$

In the opposite limit, of $\kappa \gg 1$, when $p_{eq} \approx p_0^{2/5}(\gamma a_0/\ln n)^{6/5}$ and $r_{micelle}/b \approx p_0^{2/25} n^{3/5} (\gamma a_0/\ln n)^{6/25}$

$$R_{eq}/b \approx N^{1/3} n^{4/15} p_0^{-4/75} (\gamma a_0/\ln n)^{-4/25} \tag{12}$$

For comparison purposes, R_{eq} in the $\kappa \ll 1$ limit scales as $R_{eq}/b \approx N^{3/5} p_0^{-2/5}$ for a linear string of micelles and as $R_{eq}/b \approx N^{1/2} n^{1/10} p_0^{-3/10}$ for a branched string. In the limit of $\kappa \gg 1$, the linear string size is $R_{eq}/b \approx N^{3/5} p_0^{-4/25} (\gamma a_0/\ln n)^{12/25}$ while for the branched case $R_{eq}/b \approx N^{1/2} n^{1/10} p_0^{-3/25} (\gamma a_0/\ln n)^{-9/25}$.

The single-chain configurations are qualitatively modified in the presence of free amphiphiles. Mixed micelles, consisting of both free and polymerized surfactants, begin to form once X reaches X_{cac}, the critical association concentration (cac). The fraction of polymerized surfactants within such mixed micelles, α, decreases as X increases. This, in turn, results in an increase in the number of micelles. At the same time, the overall size of the individual micelles shrinks because the number of coronal loops decreases with α. The collapsed configurations are retained over a wide X interval since B remains negative even when the number of coronal loops is small. The net result is an increase in the overall size of the globule. Denoting the total aggregation number by p, the radius of a globule comprising $m/\alpha p$ micelles of size $r_{micelle} \approx (\alpha p)^{1/5} n^{3/5} b$ is

$$R_{eq} \approx (m/\alpha p)^{1/3} r_{micelle} \approx N^{1/3} n^{4/15} (\alpha p)^{-2/15} b \tag{13}$$

The insertion of free amphiphiles into the mixed micelles ends at X_{sat}, the saturation concentration, when all mixed micelles contain a single polymerized amphiphile. The collapsed configuration unfolds completely at the immediate neighborhood of X_{sat}, when the number of loops per micelle approaches one and the bridging attraction becomes sufficiently weak.

It is convenient to analyze the interaction of polysoaps and free amphiphiles in terms of the grand canonical potential $\Omega(p,q) = (m/p)(p\epsilon_p - f\mu)$ given explicitly by

$$\Omega(\alpha,y)/mkT \approx \alpha^{-1}[\ln X_c + \gamma a_0(y^{1/3} + y^{-1/3} - 2)] + \alpha^{1/2} y^{1/2} p_0^{1/2} \ln n + (1 - \alpha^{-1}) \ln X \tag{14}$$

Here q is the aggregation number of polymerized surfactants, $f = p - q$ is the number of free, nonpolymerized surfactants per micelle, and $\mu \approx kT \ln X$ is the chemical potential of the free, unassociated surfactants. The equilibrium conditions for mixed micelles, $\partial\Omega/\partial\alpha = \partial\Omega/\partial y = 0$, lead to

$$y_{eq}^{2/3} + \kappa \alpha_{eq}^{3/2} y_{eq}^{5/6} = 1 \tag{15}$$

where $y = p/p_0$ and to

$$\frac{1}{2\gamma a_0} \ln \frac{X_c}{X} = g(y_{eq}) \equiv 1 - \frac{1}{3} y_{eq}^{-1/3} - \frac{2}{3} y_{eq}^{1/3} \tag{16}$$

The cac is determined by the requirement that $\Omega(1, u_{eq})$

$= \Omega(\alpha_{cac}, y_{cac})$. This may be written as

$$\alpha_{cac} = \frac{\ln(X_c/X_{cac}) + \gamma a_0 \Phi(u_{eq})}{\ln(X_c/X_{cac}) + \gamma a_0 \Phi(y_{cac})} \tag{17}$$

where $\Phi(x) = {}^1/_3 x^{1/3} + {}^5/_3 x^{-1/3} - 2$.

A detailed analysis of eqs 15−17 reveals two scenarios. When $\kappa > \kappa_c = 2^{1/4}$, the formation of mixed micelles involves a discrete change in both the aggregation number and α. On the other hand, when $\kappa < \kappa_c$, the insertion of free amphiphiles involves no discontinuity in the micellar characteristics. Formally, these features are traceable to eq 16. The function $g(y)$ has a maximum, $g_{max} = 1 - 2^{3/2}/3$, at $y_0 = 2^{-3/2}$. Accordingly, eq 16 has no solution when $(2\gamma a_0)^{-1} \ln X_c/X > g_{max}$ and two solutions when $(2\gamma a_0)^{-1} \ln X_c/X < g_{max}$. It has a single solution at X_0 defined by $(2\gamma a_0)^{-1} \ln X_c/X_0 = g_{max}$. For $X > X_0$ the two solutions are such that $y > y_0$ and $y < y_0$ but only the first, $y > y_0$, solution is physical. A discontinuity at X_{cac} occurs when u_{eq} of the pure intrachain micelles differs from y_{cac} of the mixed micelles at X_{cac}. Such is the case for $\kappa > \kappa_c$ when $u_{eq} < y_0$ while the mixed micelles are characterized by $y_{cac} > y_0$. Equation 17 implies that the discontinuity in the aggregation number also imposes a discrete change in α. A detailed discussion of these equations, to be found in ref 3, is beyond the scope of this article. A rough idea of the origin of these scenarios is given by the following, highly simplified, argument. Assuming that the total aggregation number, p, remains constant, the formation of mixed micelles at the cac results in a decrease in the number of free amphiphiles by $\Delta N_{surf} \approx (m/p\alpha)p(1-\alpha) = m(\alpha^{-1} - 1)$. At the same time, the total number of intrachain micelles increases by $\Delta N_{micelle} \approx (m/p\alpha) - (m/p) = (m/p)(\alpha^{-1} - 1)$. The change in total free energy of the system reflects four contributions. One penalty term is due to the loss of translational entropy of the free surfactants upon insertion into the mixed micelles, $\Delta F_{trans}/kT \approx \Delta N_{surf} \approx m(\alpha^{-1} - 1)$. The increase in the number of intrachain micelles gives rise to the second penalty term $\Delta F_{micelle}/kT \approx \Delta N_{micelle} p \bar{\epsilon}_p \approx m(\alpha^{-1} - 1)\bar{\epsilon}_p$, where $\bar{\epsilon}_p$ is the free energy per aggregated surfactant excluding the coronal contribution. These two penalty terms are compensated by two contributions favoring the formation of mixed micelles. One is the transfer free energy of the hydrophobic tails from water into the micellar core, $\Delta F_{transfer}/kT \approx -\Delta N_{surf}\delta \approx -\delta m(\alpha^{-1} - 1)$. The second is the decrease in the total coronal penalty upon formation of mixed micelles because of the corresponding decrease in the number of loops per micelle $\Delta F_{Tcorona}/kT \approx (m/p\alpha)(p\alpha)^{3/2} - (m/p)(p)^{3/2} = mp^{1/2}(\alpha^{1/2} - 1)$. At the cac the driving terms are comparable to the penalty terms. In the $\kappa \ll 1$ regime $\Delta F_{transfer}$ is dominant, leading to $m(\alpha^{-1} - 1)(1 + \bar{\epsilon}_p) \approx \delta m(\alpha^{-1} - 1)$. Since all terms exhibit identical dependence on α, there is no constraint on the allowed values assumed by α at the cac. Note that in this regime the assumption of $p \approx$ const′ is justified since $p \approx p_0$ for both mixed and pure intrachain micelles. In marked contrast, when $\kappa \gg 1$ the dominant driving term is $\Delta F_{Tcorona}$ and the condition $\Delta F_{Tcorona} \approx \Delta F_{micelle} + \Delta F_{trans}$ leads to $p^{-1/2} \sim (\alpha^{-1} - 1)/(1 - \alpha^{1/2})$. This condition imposes a definite value of $\alpha \neq 1$ at the cac. Note however that in this limit the assumption that p is constant is not valid. Rather it increases since the weakening of the coronal penalty favors micellar growth. Note further that this driving force for the insertion of free amphiphiles into the intrachain micelles is a distinctive polymeric feature.

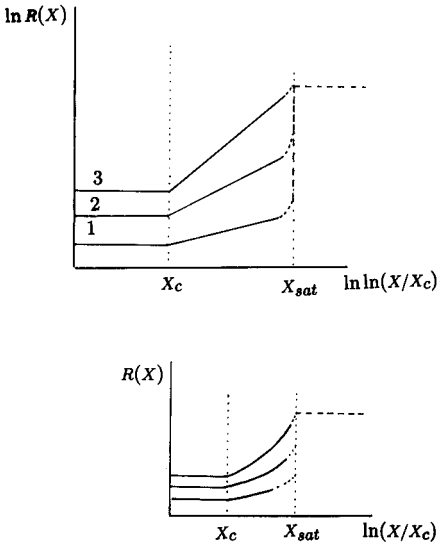

Figure 4. Swelling behavior of polysoaps as a function of the concentration of free surfactants X for the three extreme configurational scenarios: (1) collapsed globule; (2) branched string; (3) linear string.

It has no counterpart in the behavior of micelles formed by monomeric amphiphiles.

Analytical expressions for α_{eq}, y_{eq}, and X_{cac} are straightforward to obtain from eqs 15−17 in the limit of $\kappa \ll 1$.

$$\alpha_{eq} \approx \left(\frac{1}{\gamma a_0 \kappa} \ln \frac{X_c}{X}\right)^{2/3} \tag{18}$$

$$y_{eq} \approx 1 - (9/2\gamma a_0) \ln X_c/X \tag{19}$$

and

$$\ln X_c/X_{cac} \approx p_0^{1/2} \ln n \tag{20}$$

Upon substituting α_{eq} and $p \approx \alpha_{eq} p_0$ in eq 13, we obtain, to leading order

$$R_{eq}(X)/b \approx N^{1/3} n^{4/15} p_0^{-4/45} (\ln n)^{4/45} (\ln X_c/X)^{-4/45} \tag{21}$$

The swelling process of the globular state ends around X_{sat} obtained from (18) by setting $\alpha_{eq} \approx 1/p_0$, leading to

$$\ln X_c/X_{sat} \approx p_0^{-1} \ln n \tag{22}$$

Since eq 18 is only valid while the number of loops is much larger than one, this estimate of X_{sat} is actually rather rough. Substituting X_{sat} in eq 13 gives a rough idea of the maximal swelling while the polysoap is in a globular state

$$R_{eq}(X_{sat})/b \approx N^{1/3} n^{4/15} \tag{23}$$

and the corresponding swelling ratio $R_{eq}(X_{sat})/R_{eq}(X_{cac}) \approx p_0^{2/15}$. The intriguing feature of this scenario is that the globular state is expected to unfold completely (Figure 4) when the number of loops per micelles is one or less. Thus, in a narrow concentration range around X_{sat} the chain will eventually attain a dimension of $R_{eq}/b \sim N^{3/5}$. This final, fully unfolded, state is achieved by all polysoaps irrespective of their initial configuration.

It is instructive to compare the maximal swell ratio of polysoaps for different initial configurations. We

focus on the case of long polysoaps forming strings of micelles. The maximal swelling ratio in the following is defined as $\omega = N^{3/5}b/R_{eq}(\alpha=1)$. For the collapsed globule scenario $\omega \approx N^{4/15}n^{-4/15}p_o^{2/15}$ when $\kappa \ll 1$ and $\omega \approx N^{4/15}n^{-4/15}p_0^{4/75}(\gamma a_0/\ln n)^{4/25}$ for $\kappa \gg 1$. A linear string of micelles in the $\kappa \ll 1$ regime is characterized by $\omega \approx p_0^{2/5}$ while in the opposite limit $\omega \approx p_0^{4/25}(\gamma a_0/\ln n)^{12/25}$. Finally, in the random branching scenario $\omega \approx N^{10}n^{-1/10}p_0^{3/10}$ for $\kappa \ll 1$ and $\omega \approx N^{1/10}n^{-1/10}p_0^{3/25}(\gamma a_0/\ln n)^{9/25}$ in the $\kappa \gg 1$ limit. Altogether, the dependence of ω on N, n, and p_0 in the various cases is markedly different. This suggests ω as a diagnostic tool for the characterization of the configurations of isolated polysoaps.

V. Discussion

Internal aggregation of the type considered occurs in a wide variety of systems including multiblock copolymers[23] and graft copolymers[24] such as hydrophobically modified water-soluble polymers. The qualitative conclusions obtained in this article apply to all such systems. However, the case of polysoaps interacting with chemically identical monomeric amphiphiles is especially convenient to model and analyze. It also affords the benefit of having micelles formed by the monomeric amphiphiles as a natural reference system. Our discussion suggests that titration of dilute polysoaps with solutions of monomeric amphiphiles affords a useful probe for the configurations adopted by the polysoaps. In particular, the details of the $R(X)_{eq}$ *vs* X curves and the maximal swelling ratio, ω, should allow one to distinguish between the extreme three scenarios discussed in this article and in ref 3. The case of polysoaps exhibiting equilibrium characteristics due to bridging is especially striking. In such a system the polymers retain their collapsed globule configuration over a wide range of surfactant concentrations. A complete unfolding then takes place over a narrow range of X. It is however important to bear in mind that kinetic effects may play an important role in determining the configurations adopted by the isolated polysoaps. Sample preparation, incubation times, *etc.* may thus have strong effect on the realized configurations. This behavior is markedly different from that of flexible homopolymers whose configurations are determined solely by the solvent quality. This distinctive behavior is traceable to the multiple minima exhibited by the free energy surface describing the configurations of the chain. From a different perspective this complication does have an attractive side. As noted in the Introduction, the secondary/tertiary structure exhibited by polysoaps is suggestive of proteins. Actually, the phenomenological similarity between these two families of polymers extends further since both undergo surfactant induced denaturation, form gels *etc.* However, the fact that both species are characterized by a "rugged" free energy surface[25] suggests that there may be a deeper similarity between them.

Acknowledgment. The authors benefited from instructive discussions with D. Leckband and P. Goldbart. This work was carried out while O.V.B. enjoyed the hospitality of K. Binder and financial support from the Alexander von Humboldt foundation.

References and Notes

(1) (a) Bader, H.; Dorn, K.; Hupfer, B.; Ringsdorf, H. *Adv. Polym. Sci.* **1985**, *64*, 1. (b) Gros, L.; Ringsdorf, H.; Scupp, H. *Angew. Chem., Int. Ed. Engl.* **1981**, *20*, 305. (c) Laschewsky, A. *Adv. Polym. Sci.*, in press. (d) Hogen-Esch, T. E.; Amis, E. *Trends Polym. Sci.* **1995**, *3*, 98. (e) Glass, J. E., Ed. *Polymers in Aqueous Media: Performance Through Association;* American Chemical Society: Washington, DC, 1989.
(2) (a) Iliopoulos, I.; Olsson, U. *J. Phys. Chem.* **1994**, *98*, 1500. (b) Valint, P. L.; Bock, J. *Macromolecules* **1988**, *21*, 175. (c) Biggs, S.; Hill, A.; Selb, J.; Candau, F. *J. Phys. Chem.* **1992**, *96*, 1505. (d) Strauss, U. P.; Layton, L. H. *J. Phys. Chem.* **1953**, *57*, 352.
(3) Borisov, O. V.; Halperin, A. *Langmuir* **1995**, *11*, 2911.
(4) Gan, L. M.; Yeoh, K. W.; Chew, C. H.; Koh, L. L.; Tan, T. L. *J. Appl. Polym. Sci.* **1991**, *42*, 225 and references quoted therein.
(5) (a) Halperin, A.; Zhulina, E. B. *Europhys. Lett.* **1991**, *16*, 337. (b) Halperin, A.; Zhulina, E. B. *Prog. Colloid Polym. Sci.* **1992**, *90*, 156. (c) Zhulina, E. B.; Halperin, A. *Macromolecules* **1992**, *25*, 5730.
(6) Zhulina, E. B. *Macromolecules* **1993**, *26*, 6273.
(7) Misra, S.; Varanasi, S. *Macromolecules* **1993**, *26*, 4184.
(8) (a) Halperin, A.; Williams, D. R. M. *Macromolecules* **1993**, *26*, 6652. (b) Halperin, A.; Williams, D. R. M. *Phys. Rev. E* **1994**, *49*, R986.
(9) Semenov, A. N.; Subotin, A. V. *Soc. Phys.—JETP (Engl. Transl.)* **1992**, *74*, 660.
(10) Milner, S. T.; Witten, T. A. *Macromolecules* **1992**, *25*, 5495.
(11) Matsen, M. *J. Chem. Phys.*, in press.
(12) Semenov, A. N.; Joanny, J. F.; Khokhlov, A. R. *Macromolecules* **1995**, *28*, 1066.
(13) Israelachvili, J. N. *Intramolecular and Surface Forces*, 2nd ed.; Academic Press: London, 1991.
(14) Daoud, M.; Cotton, J. P. *J. Phys. (Paris)* **1982**, *43*, 531.
(15) Birshtein, T. M.; Zhulina, E. B. *Polymer* **1984**, *25*, 1453.
(16) Halperin, A.; Tirrell, M.; Lodge, T. P. *Adv. Polym. Sci.* **1990**, *100*, 31.
(17) Halperin, A. In *Soft Order in Physical Systems*; Bruinsma, R., Rabin, Y., Eds.; NATO ASI Series 323, Series B, Physics; Plenum: New York, 1994.
(18) Witten, T. A.; Pincus, P. A. *Macromolecules* **1986**, *19*, 2509.
(19) Grest, G. A.; Kremer, K.; Milner, S. T.; Witten, T. A. *Macromolecules* **1989**, *22*, 1904.
(20) Dan, N.; Tirrell, M. *Macromolecules* **1992**, *25*, 2890.
(21) Wijmans, C. M.; Zhulina, E. B. *Macromolecules* **1993**, *26*, 7214.
(22) (a) Halperin, A. *Europhys. Lett* **1989**, *8*, 351. (b) Halperin, A.; Alexander, S. *Macromolecules* **1989**, *22*, 2403.
(23) Halperin, A. *Macromolecules* **1991**, *24*, 1418.
(24) Birshtein, T. M.; Borisov, O. V.; Zhulina, E. B.; Khokhlov, A. R.; Yurasova, T. A. *Polym. Sci. USSR (Engl. Transl.)* **1987**, *29*, 1169.
(25) See, for example: Karplus, M.; Shaknovich, E. In *Protein Folding*; Creighton, T. E., Ed.; Freeman: New York, 1994.

MA951565W